Climate Change Induced Morphological Response Assessment in Estuary: Case Study of Arakawa River Mouth, Niigata, Japan

Kota Ohizumi (k.oizumi3025@gmail.com)
Niigata University: Niigata Daigaku https://orcid.org/0000-0001-5817-3148
Ryota Nakamura
Niigata University: Niigata Daigaku
Kunihiko Ishibashi
Niigata University: Niigata Daigaku

Research Article

Keywords: Estuary, Morphological change, Pseudo Global Warming method, WRF-Hydro, XBeach, Flood term

Posted Date: April 7th, 2022

DOI: https://doi.org/10.21203/rs.3.rs-1433381/v1

Abstract

Morphological responses in estuaries are assumed to change in the future in association with changes in tidal levels, waves, and discharges under climate change. This study proposes a numerical modelling system for morphological changes in local estuaries to simulate hindcast and future scenarios considering futuristic tidal levels, waves, and discharges. The numerical modelling system configuration was based on three models: Weather Research and Forecasting model Hydrological modelling system (WRF-Hydro), Simulating WAves Nearshore (SWAN), and eXtreme beach behavior (XBeach). SSP5-8.5 and RCP8.5 were selected for constructing global warming environmental fields using the pseudo global warming (PGW) methodology. We conducted a numerical simulation of the morphological changes at the mouth of the Arakawa River during flood season. The hindcast simulation quantitatively reproduced the post-flood event sandbar topography by using boundary conditions of the simulated wave and observed discharge rate. Additionally, sea level rise, decrease in significant wave heights and mean wave periods, and increase in discharges were simulated for future simulations of the Arakawa River under climate change. The results considering future scenarios elucidated that characteristics of morphological responses changed compared with that of the present climate. Particularly, climate change enhanced the erosion effects since overflow due to rise in water level was more likely to occur at the river mouth sandbars. Hence, we suggest that the morphological response of estuaries to complex physical fields is sensitive to external force changes under climate change conditions.

1. Introduction

The topography of estuaries is highly vulnerable to various external forces such as tides, waves, and discharge (Harris et al. 2002; Dalrymple and Choi 2007). Therefore, the influential factors and mechanisms for topography formation in estuaries have been analyzed in various studies (e.g. Edmonds and Slingerland 2007; De Swart and Zimmerman 2009; Van der Wegen and Roelvink 2012; Leonardi et al. 2013; Guo et al. 2014; Nienhuis et al. 2016). Further, topographical changes can be predicted in estuaries since future variations in external forces influencing morphological changes are assumed be in accordance to the IPCC report.

Generally, climate change impact assessments of tide level, waves, and discharge have been performed, which are the main external forces influencing the morphological changes in estuaries. Global sea level rise is expected as a result of the thermal expansion of water and melting glaciers in coastal zones under climate change (Church et al. 2013). In addition, wave fields are presumed to change globally in the future as significant wave heights and mean wave periods vary by 5–15 % (Morim et al. 2019). In river basins under climate change, increases in atmospheric water vapor owing to rising temperatures cause intense precipitation events (Trenberth. 2011). Furthermore, global flood risk assessments analyze regional variations in the characteristics of this change (Hirabayashi et al. 2013; Arnell and Gosling 2016). Mori et al. (2021) summarized recent studies on climate change impact assessments around Japan on ocean waves, storm surges, precipitation, and discharge. Based on these global assessments, we expect to evaluate the futuristic impact of global warming on a regional scale.

Significant attempts have recently been made to predict future morphological responses to these climate change assessments. In particular, sea level rise affects shoreline changes, and the erosion trend of sandy coastlines has been estimated worldwide, except in some regional areas (Vousdoukas et al. 2020). According to regional assessment, sandy beaches around Japan are eroded by sea level rise (Udo and Takeda 2017; Mori et al. 2018). Furthermore, shoreline change assessments are expected to become more sophisticated as methods other than the Bruun rule (Bruun 1962) have been proposed, such as a probabilistic coastline recession (PCR) model (Ranasinghe et al. 2012; Le Cozannet et al. 2019; Dastgheib et al. 2021).

However, the morphological responses of estuaries and tidal inlets are not well studied in the context of future scenarios. Some studies have conducted impact assessments on estuaries and tidal inlets and have considered the relative sea level rise (Dissanayake et al. 2012) and topographical features (Leuven et al. 2019). Ranasinghe et al. (2013) emphasized the importance of considering the impacts of rainfall, runoff, as the Bruun effect alone are not enough. Based on this study, assessments using local-scale modelling under the expected future climate have been conducted (Ranasinghe 2016; Duong et al. 2016, 2017, 2018). However, insufficient studies have assessed estuarine climate change impacts while considering multiple external forces. In particular, few studies have focused on short-term events, although some studies have evaluated them over a long-term scale.

Therefore, this study proposes a new numerical modelling system for morphological changes in estuaries during short-term events that can simulate hindcast and future scenarios. This numerical modelling system consists of several open-source models, observational data, and results of the general circulation models (GCM) under future scenarios. The pseudo global warming (PGW) method (Sato et al. 2006; Kimura and Kitoh 2007) was used to simulate meteorological conditions under climate change. Previous studies have also used PGW fields to assess the impact of meteorological phenomena (Nakamura et al. 2016, 2020; Mäll et al. 2020; Nakamura and Mäll 2021). Additionally, we used the aforementioned numerical modelling system to assess the impact of the present climate and climate change on the Arakawa River mouth during a flood event in the monsoon season of 2018. The external forces simulated by the PGW method were used as the driving forces to simulate morphological response in the numerical simulation of climate change. Finally, based on the numerical results, we discuss morphological characteristics of the Arakawa River mouth under the expected future climate conditions.

There are some aforementioned previous studies addressing the long-term evaluation of morphological changes in estuary under climate change. However, few studies have assessed estuarine climate change impacts while considering multiple external forces especially under short term extreme event. Therefore, this study could provide in-depth understanding of sensitivity of morphological changes in estuary associated with the extreme events under climate change based on pseudo global warming method.

2. Material And Methods

2.1 Study area

Significant morphological changes occur throughout the season at the mouth of the Arakawa River in Niigata, Japan (Figure 1). As a general topographic trend in the Arakawa River mouth, the river mouth opens in Baiu from spring to summer because of high discharge events and closes in the winter season due to intermittent high waves (Ohizumi et al. 2021). Moreover, the opened river mouth affects the brackish environment due to saltwater intrusion, whereas the closed river mouth increases the flood risk since the sandbar causes the water level to rise. Consequently, maintenance of the river mouth must be flexible and adaptable to topographical features. Therefore, the Ministry of Land, Infrastructure, Transport, and Tourism (MLIT) has been carrying out maintenance, including regular monitoring and excavation of sandbars before the flood period to reduce the water level. Hence, it is important to understand the future characteristics of sandbars under climate change conditions in this area.

This study focused on the flood term caused by the rapid increase in discharge rate at the Arakawa River mouth in 2018 (Figure 1 (c)). In particular, the topography of the river mouth sandbar was differed from April 27 to May 21, which is illustrated by aerial photogrammetry. The maximum discharge rate of 2063.27 m^3/s at 20:00 UTC on May 17 was observed at Tsudurayama stream gauging station in the Water Information System (WIS) of MLIT. This was because a heavy rainfall event occurred from May 17–19, which was caused by the Baiu front. Therefore, the MLIT conducted field surveys before and after a high discharge event at the mouth of the Arakawa River. In addition, land area was measured on April 27 and May 21 and sea area was measured on May 1, 2, 8 and May 29, 30, respectively. Field survey data were used as the initial boundary conditions for numerical simulations, and the numerical simulation term was set to approximately one month to fully cover the field survey period.

2.2 Model descriptions

Figure 2 shows the configuration of the numerical modelling system. In this study, we used the following three numerical simulation models: Weather Research and Forecasting model Hydrological modelling system (WRF-Hydro) (Gochis et al. 2015), Simulating WAves Nearshore (SWAN) (Booji et al. 1999) and eXtreme Beach behavior (XBeach) (Roelvink et al. 2009). In addition, these configurations do not consider interactions between WRF-Hydro, SWAN, and XBeach.

WRF-Hydro is a hydrological model expanded from the Weather Research and Forecasting (WRF) model (Skamarock et al. 2008), and simulates the physical processes of the atmosphere, land surface, and hydrology. SWAN is a third-generation wave model based on the wave action balance equation, which simulates the significant wave height (Hs) and mean wave period (TM01). XBeach is a process-based nearshore morphology model that considers hydrodynamic and morphodynamic processes. As a hydrodynamic process, XBeach has two representative modes: surf beat mode and nonhydrostatic mode. The surf beat mode was solved using the wave action balance equation and nonlinear shallow water equations. In contrast, morphodynamic processes were solved by the advection-diffusion equation for sediment transport and formulation for bottom updating.

Numerical simulations under the present climate were conducted, and is illustrated by the black arrows in Figure 2. First, we developed the initial boundary conditions using WRF Preprocessing System (WPS) based on GFS-FNL provided by the National Centers for Environmental Prediction (NCEP), and WRF-Hydro simulates hydro-meteorological conditions including wind velocity, precipitation, and runoff employed for XBeach modelling. Moreover, the elevation boundary condition is the topographical data obtained from the Japan Flow Direction Map (J-FlwDir; Yamazaki et al. 2018). Second, SWAN simulates the wave spectral density using the wind velocity forecasted by WRF-Hydro and bathymetry data obtained from GEBCO2019 (Sandwell et al. 2014). Finally, XBeach simulates the morphological changes at the Arakawa River mouth using the wave spectral density forecast by SWAN, observed data available to the public, and field survey data of MLIT. The discharge boundary condition was the discharge rate data of the Tsudurayama stream gauging station provided by the WIS. In addition, the tide boundary is the astronomical tide data of the Nezugaseki tide station located approximately 50 km northeast, which was provided by the Japan Meteorological Agency (JMA).

Numerical simulations under climate change were conducted as indicated by the red arrows in Figure 2. Although the initial boundary conditions are different, the procedure is the same as that for the hindcast simulation. Future simulations will calculate the external forces under climate change using the PGW method. First, we created the initial boundary conditions based on the climate change scenario, namely, the CMIP6 and CMIP5 multi-model ensembles. The PGW fields of surface temperature (ST), atmospheric temperature (AT), relative humidity (RH), and geopotential height (GPH) are used to calculate the meteorological data which are the boundary conditions for numerical simulations by WRF-Hydro. In addition, the sea level change was considered for the boundary conditions of the numerical simulations by SWAN and XBeach. Here, sea level change is assessed by the local sterodynamic sea level change based on ocean dynamic sea level change and global mean thermosteric sea level rise (Gregory et al. 2019). Second, discharge is calculated using the runoff obtained under the present and future climates. Finally, the morphological change under climate change at the Arakawa River mouth was evaluated by numerical simulations using XBeach, with the boundary conditions of tidal level, waves, and discharge estimated by future scenarios.

2.3 Boundary conditions under climate change

We conducted climate change impact assessments using CMIP6 models under the Shared Socioeconomic Pathways (SSPs) scenario. CMIP6 models were used because they have been reported to perform better than CMIP5 models (Kim et al. 2020; Fan et al. 2020). Furthermore, we also conducted climate change impact assessments using CMIP5 models under the Representative Concentration Pathways (RCPs) scenario. This was because RCP scenarios have been used in many previous studies. Each scenario was selected as SSP5-8.5 (SSP585) and RCP8.5 (RCP85), which are the most extreme scenarios. In previous studies, PGW sensitivity experiments under RCP8.5 which used the CMIP5 model were used for climate change impact assessments (Nakamura et al. 2016, 2020; Mäll et al. 2020; Nakamura and Mäll 2021). In the present study, numerical simulations under climate

change conditions were conducted using the PGW method with 25 and 18 multi-model ensembles of CMIP6 and CMIP5, respectively. The PGW fields were constructed using the monthly mean value difference between the future (2081–2100) and the present period (2015–2024). The construction method of the PGW fields is same as that of Nakamura and Mäll (2021). Tables S1 and S2 show the CMIP6 and CMIP5 models used by each multi-model ensemble.

Figure 3 shows PGW fields of ST, AT, RH, and GPH in May. ST generally rises around Japan, and especially over land. AT, RH, and GPH evaluate at 500 hPa height. Generally, AT increases, RH decreases, and GPH increases throughout Japan. Specifically, as the mean of a plane distribution, AT increased by 4.591 and 4.033 °C in SSP585 and RCP85, respectively. Further, RH decreased by 1.983 and 1.540 % in SSP585 and RCP85, respectively. Meanwhile, GPH increased by 92.525 and 76.688 m in SSP585 and RCP85, respectively. Therefore, the planar trend of PGW fields between SSP585 and RCP85 is similar, although SSP585 shows more pronounced global warming than RCP85.

Sea level changes around the Sea of Japan were evaluated from sterodynamic sea level changes (Gregory et al. 2019). Formulation of the sterodynamic sea level change is as follows:

(ΔZ=Δζ+η (1)

where ΔZ is the hemodynamic sea level change, ΔZ is the ocean dynamic sea level change, and is the global mean thermosteric sea level rise. This was obtained from the CMIP6 and CMIP5 data variables zos and zostoga. Furthermore, the evaluation range of the sterodynamic sea level change was same as the numerical simulation range of SWAN.

Figure 4 shows sea level change of each GCMs from 2015–2100 and difference between future (2081–2100) and present (2015–2024) periods in May. According to results of each multi-model ensemble, sterodynamic sea level around the Sea of Japan is exhibiting a rising trend. In addition, the planar trend of sea level change between scenarios also is similar as that of the PGW fields although the model bias of RCP85 is larger than that of SSP585. Further, the mean value of sea level rise is 0.33 and 0.39 m in SSP585 and RCP85, respectively, within the target area.

2.4 Setting numerical models

Sensitivity analysis was performed using different microphysics schemes in the physical models of WRF-Hydro. This is because many sensitivity studies on precipitation using WRF have illustrated the sensitivity of microphysics schemes to precipitation simulations (Liu et al. 2011; Avolio and Federico 2018; Mohan et al. 2018; Jeworrek et al. 2021). In this study, the microphysics schemes selected were WRF Single-Moment 5-class (WSM5; Hong et al. 2004), WRF Single-Moment 6-class (WSM6; Hong et al. 2006), and Thompson scheme (Thom; Thompson et al. 2008). Furthermore, hydrological simulation in WRF-Hydro is parameterized for various hydrological processes. Thus, this sophisticated study uses the parameter estimation tool (PEST) to automatically determine the parameter settings (Wang et al. 2019). However,

the parameters were uniform in all cases since our study aims to elucidate changes in the present and future climate. Other physical models were simulated in a unified manner in the numerical simulations of WRF-Hydro, SWAN, and XBeach.

As the main setting of the numerical model, WRF-Hydro performs hydrological calculations in domain 3, which includes the Arakawa River basin. Furthermore, WRF-Hydro does not activate the baseflow model in order to explicitly show the runoff impact. XBeach activates the discharge option shown in the manual (XBeach Documentation, 2017). This allows for discharge from the river boundary in the XBeach model. In addition, this study did not consider sediment supply from the upper reaches of the river. For the simulation of XBeach, the grain sizes of D_{50} and D_{90} were set to 0.370 and 0.830 mm, respectively, which were obtained from a field survey (Ohizumi et al. 2021).

Table 1 lists the results of numerical simulations. In this study, cases with physical fields based on different microphysics schemes are denoted as WSM5, WSM6, and Thom. In addition, cases based on climate change scenarios are denoted as SSP585 and RCP85. Here, the numerical simulation of XBeach under future climate conditions evaluated the morphological responses based on tide level, waves, and discharge under climate change. Therefore, for case studies of XBeach, we conducted cases based on sea level rise (SLR), waves under climate change (WC), and discharge under climate change (DC). Details of the DC scenarios are described in the results under future climate conditions in Section 3.2.

3. Results

3.1 Numerical simulation under present climate

WRF-Hydro numerically simulated wind velocity, precipitation, and runoff. Figure 5 (a) shows the simulated cumulative precipitation and runoff. The simulated cumulative precipitation was compared with the observed cumulative precipitation in the Arakawa River Basin. Hence, the WSM5 and WSM6 cases simulated a rapid increase in precipitation during periods of increased observed precipitation, whereas the simulated precipitation was underestimated. The same trend was simulated for runoff in the WSM5 and WSM6 cases. Therefore, the simulated results for the WSM5 and WSM6 cases suggest that the reproduction of flood events is somewhat underestimated.

Wave fields simulated by SWAN in the Sea of Japan and hindcast simulation were quantitatively validated around the values obtained by two observed points (NOWPHAS) close to the Arakawa River mouth. Wave simulations were carried out using wind fields of the WSM5 and WSM6 cases, which simulated rapid runoff. Figure 5 (b) shows the simulated results for significant wave heights (Hs) and mean wave periods (TM01). The correlation coefficient (R) and root mean square error (RMSE) of Hs were above 0.75 and about 0.25–0.50 m, respectively. In contrast, R and RMSE of TM01 were above 0.50 and about 1.20–1.70 s, respectively. Hence, we considered that the simulated wave fields around Japan were reliable.

Finally, XBeach simulated the morphological changes at the Arakawa River mouth during the flood term. Figure 5 (c) shows the initial boundary conditions and hindcast simulations of WSM5 and WSM6; both cases simulated morphological changes. In particular, the topography of the river mouth sandbar was similar to that of aerial photographs (Figure 1 (c)). Therefore, we conducted a quantitative validation of the cross-shore (C1–C4) and alongshore (A1) elevation lines using the Brier Skill Score (BSS; Van Rijn et al. 2003; Sutherland et al. 2004), which is illustrated in Figure 5 (c). The BSS was estimated using the following equation:

$$\mathrm{BSS} = 1 - \frac{\sum\left(z_{fin} - z_{sim}\right)^2}{\sum\left(z_{fin} - z_{ini}\right)^2}$$

where is the initial bed level before morphological changes, is the observed bed level after morphological changes, and is the simulated bed level after morphological changes. Table 2 shows quantitative assessment of the BSS (Sutherland et al. 2004) and results for each line. The BSS for both cases showed good values in lines with large morphological changes (C1, C4, and A1 lines) and poor values in C2 and C3 lines. The poor values in lines C2 and C3 can be attributed to the hindcast simulation which could not simulate minor morphological changes on the sea side. However, we considered that the hindcasts were reliable in assessing the open characteristics since the BSS had good values for C1, C4, and A1.

3.2 Numerical simulation under future climate

We conducted climate change impact assessments for external forces that induce morphological changes at the mouth of the Arakawa River. Figure 6 (a) shows the difference in cumulative precipitation between the future and present climate. All future scenario cases were confirmed to have an increase in cumulative precipitation around the Sea of Japan during the study period. This is probably because the amount of water vapor capacity in the air has increased due to global warming, which has also been described in a previous study (Trenberth 2011). In addition, Osakada and Nakakita (2018) indicated that heavy rainfall events will occur frequently in the future around the Sea of Japan side during the Baiu season, which is the same period as the present study. Therefore, we suggest that flood risk in the Arakawa River Basin increases during the Baiu season under climate change due to heavy rainfall.

The simulated runoff for the future and present climates at the Tsudurayama stream gauging station is also shown (Figure 6 (b)). The runoff under future scenarios was also simulated to increase owing to increased precipitation in the Arakawa River basin. Previous studies conducted on a global scale have shown a similar increasing trend in flood risk in Japan (Hirabayashi et al. 2013; Arnell and Gosling 2016). As regional-scale studies in Japan, Kobayashi et al. (2020) have stated from future assessments throughout Japan basins that large-scale discharge is an increasing trend on the Sea of Japan side. In addition, certain rivers in Japan (Nagara River) have exhibited an increase in discharge by 33 % under climate change (Harada et al. 2020). In summary, we presumed that the flood risk in the Japanese river basin would increase under climate change based on the results of the present study.

We conducted three case studies under climate change conditions based on the simulated runoff of the WSM6 cases. The three future scenarios (DC1–DC3) were derived from the simulated results of the total and maximum runoff and observed discharge (Table 1). In case of DC1, the total runoff was simulated to be 20882.52 and 23915.43 m^3/s for WSM6 and WSM6-SSP585, respectively. Hence, the observed discharge rates for the all periods were multiplied by its multiplier of 1.15. For DC2, the maximum runoff was simulated to be 1219.65 and 1710.69 m^3/s for WSM6 and WSM6-SSP585, respectively. Therefore, the maximum observed discharge at 20:00 (UTC) on May 17 was added by its difference of + 491.04 m^3/s. For DC3, the maximum runoff was simulated to be 1219.65 and 1253.95 m^3/s for WSM6 and WSM6-RCP85, respectively. Hence, the maximum observed discharge at 20:00 (UTC) on May 17 was added by its difference of + 34.30 m^3/s. These future scenarios are comparable to those in studies that have assessed discharges in Japan (Kobayashi et al. 2020; Harada et al. 2020). However, these are tentative scenarios for increased discharge in the Arakawa River during the Baiu season. Thus, it is important to select scenarios that eliminate uncertainty in the future since regional scale climate change impact assessments remain challenging (Xie et al. 2015).

Subsequently, we evaluated the wave fields under climate change by analyzing the differences in Hs and TM01 between the future and present climate (Figure 7). In the target period, Hs and TM01 simulated a decreasing futuristic trend around the Sea of Japan side. To explain this, we considered that wind speed simulated by WRF-Hydro decreases around the Sea of Japan side (Figure S1). Previous studies have also confirmed decrease in significant wave heights and mean wave period around Japan under the RCP8.5, which is consistent with the results of this study (Morim et al. 2019; Shimura and Mori 2019). Therefore, we considered that the results of the climate change impact assessment of wave fields are reliable, and the wave fields under climate change are used as the initial boundary conditions for XBeach under future scenarios.

Finally, we assessed case studies simulated by XBeach in estuarine morphology under climate change conditions. Figure 8 shows the numerical simulation results of the case employing WSM6 for micro physics scheme in WRF-Hydro. In SSP585-SLR, SSP585-SLR-WC, and RCP85-SLR-WC-DC3, morphological changes were simulated in the same areas as in the hindcast case (around the C1 and C4 lines illustrated in Figure 5 (c)), although there was some flushing. As a feature of these cases, the discharge boundary condition in XBeach was almost the same as the observations. In contrast, severe erosion occurred over the entire river mouth sandbar in the cases of SSP585-SLR-WC-DC1 and SSP585-SLR-WC-DC2. In both cases, the maximum discharge under the discharge boundary condition significantly increased. Therefore, this elucidates that the morphological response is highly dependent on the maximum discharge of river flow.

4. Climate Change Impact Assessments On Morphological Change

Impact of climate change was analyzed based on the deformation process of the river mouth sandbar. Figure 9 shows the numerical simulation results, which focus on the river mouth sandbar. In Figure 9 (a), the hindcast case shows that the morphological changes during a month occurred during a short flood

term, which is why the changes were simulated between 18:00 and 21:00 on May 17. The physical phenomenon at this time is overflow from the river to the sea at the relatively low sandbar due to rise in water level on the river side. Consequently, we considered that the morphological changes were caused by rapid increase in water velocity over the sandbar on the seaside during overflow. Moreover, SSP585-SLR-WC-DC1 was simulated based on the morphological change of the entire sandbar between 18:00 and 21:00 on May 17. This is because overflow occurred on the entire sandbar, as the maximum discharge was higher than the observed value. To indicate that overflow occurs in the severely eroded area. Figure S2 shows the bed level and water level of each line in the maximum discharge.

For further analysis, we assessed characteristics of morphological changes of the sandbar along the alongshore direction (as shown in Figure 9 (b), A1 line illustrated in Figure 5 (c)). First, as the impact of sea level rise is assessed, the sandbar in the case of SSP585-SLR was flushed more than in the present climate. The results numerically suggest that the sandbar is prone to be overflowed in the case considering sea level rise of 0.33 m. Here, Dissanayake et al. (2012) pointed out that the long-term simulation of inlet over a period of approximately 100 years shows decrease in land area when sea level rise is considered. In this study, we also found that sea level rise causes severe erosion in land areas when floods are generated. Second, upon impact assessment of oceanic surface waves under climate change, we found that the morphological response varied in case of SSP585-SLR-WC. Since overflow is the main factor in flood events, we implied that the effect of waves is smaller than that of sea level rise and discharge changes.

Finally, the impact of climate change on discharge was assessed from the cases using the future discharge scenarios (DC1–DC3). The results of this flood event had a significant impact on the morphology caused by increase in discharge. Particularly, in case of SSP585-SLR-WC-DC1 and SSP585-SLR-WC-DC2, a significant reduction was simulated in the land area of the sandbars which was mainly attributed to an increase in the maximum discharge (Figure 9 (c)). Since the trend is mainly due to the maximum discharge, we concluded that consideration of the maximum discharge is important to evaluate the flush of the sandbar under climate change. Furthermore, whether overflow occurs is the main factor in this major morphological response; hence, it is necessary to consider the effect of the initial topography. Therefore, we presumed that case studies of any maximum discharge and initial topography are important for a sophisticated assessment of the morphological responses in future flood terms.

In conclusion, climate change impact assessments on the morphological changes in the Arakawa River mouth during Baiu season can be summarized as follows. The first is the increased risk of severe erosion due to sea level rise. Specifically, the estuarine environment in the water level rise increases the likelihood of overflow on sandbars. Therefore, we implied that overflows occur more frequently under the consideration of sea level rise. The second is the assessment of maximum discharge of the Arakawa River under climate change. Discharges in the Arakawa River suggest an increasing trend in the future Baiu season, which is in accordance with a previous study that indicated an increase in heavy rainfall events during the Baiu season (Osakada and Nakakita. 2018). Based on these two conclusions, we presumed that the Arakawa River mouth under climate change would be more eroded during the flood

term if the same topography could be constructed at the river mouth in the future. It is noteworthy that the long-term changes in initial topography of the river mouth before the flood season cannot be considered in this study and future research is encouraged in this direction.

5. Conclusions

In this study, we propose a numerical modelling system to assess the impact of climate change on morphological changes in estuaries. Furthermore, the numerical system was applied to case studies under future scenarios at the Arakawa River mouth in the flood term for one month. The conclusions of the numerical simulations are as follows.

This numerical modelling system was constructed and simulated by considering external forces, such as tide level, waves, and discharge, acting on the topography of the estuary. The hindcast simulations significantly simulated the topographic characteristics of flushing on the Arakawa River mouth sandbars. Next, a numerical simulation of future scenarios was conducted using the PGW method. As a result, the coastal area around Arakawa River mouth numerically showed a rise in sea level of 0.33 and 0.39 m in SSP585 and RCP85, respectively, and decrease in significant wave heights and mean wave periods. Moreover, the Arakawa River Basin showed an increase in discharge with increasing precipitation. Based on these changes in the external forces under climate change, we numerically confirmed that the morphological response varied between future cases.

Detailed analysis suggested that sea level rise and increased discharge intensify the erosion action at the river mouth during the flood term. This is because the water level rise creates an environment where overflow from the river side to the sea side is more likely to occur on the river mouth sandbar. Thus, the erosion action was enhanced when the case with 0.33 m sea level rise was considered. When the maximum discharge increased, morphological changes occurred over the entire river-mouth sandbar. Consequently, it was numerically shown that external forces under climate change have a significant impact on the morphological response in estuaries.

Future studies should conduct more case studies on the morphological changes in estuaries under climate change, while bearing in mind the uncertainties of regional-scale climate change impact assessments (Xie et al. 2015). These tasks were also considered by the results of morphology simulations at the river mouth to change the external forces under climate change in this study. Furthermore, Duong et al. (2016) also stated that the small tide inlet is a high-priority research area since it is vulnerable to climate change. Therefore, the development and upgradation of modelling approaches, including long-term morphological changes under climate change, for sustainable estuary maintenance is a future challenge.

Declarations

Acknowledgements

We acknowledge the Uethu River and National Highways Office, Hokuriku Regional Development Bureau, the Ministry of Land, Infrastructure, Transport, and Tourism (MLIT) for providing us with field survey data from the Arakawa River mouth. We acknowledge the River Foundation from public interest incorporated foundation and the Japan Society for the Promotion of Science for funding. We would like to thank Editage (www.editage.com) for English language editing.

Ethical Approval

This study does not require ethics committee approval with human and animal subjects.

Consent to Participate

Not applicable.

Consent to Publish

Not applicable.

Authors Contribution

Kota Ohizumi and Ryota Nakamura contributed to the conceptualization, design and methodology of this study. Kota Ohizumi and Kunihiko Ishibashi contributed to the formal analysis. Kota Ohizumi contributed to the numerical simulation, validation, visualization and writing original draft. Ryota Nakamura contributed to the funding acquisition and review of the original draft.

Funding

This study received the financially support from the River Foundation, public interest incorporated foundation (Grant numbers: 2020-5311-004). Further, this study received the Grant-in-Aid for Early-Career Scientists from the Japan Society for the Promotion of Science (Grant numbers: 19K15098).

Competing Interests

The authors declare no competing interests in this study.

Availability of data and materials

The datasets in this study are available from the corresponding author on reasonable request.

References

1. Arnell NW, Gosling SN (2016) The impacts of climate change on river flood risk at the global scale. Clim Chang 134(3): 387-401. https://doi.org/10.1007/s10584-014-1084-5
2. Avolio E, Federico S (2018) WRF simulations for a heavy rainfall event in southern Italy: Verification and sensitivity tests, Atmos Res 209(1): 14-35. https://doi.org/10.1016/j.atmosres.2018.03.009

3. Booji N, Ris RC, Holthuijsen LH (1999) A third-generation wave model for coastal regions: 1. Model description and validation. J Geophys Res: Ocean 104(C2): 7649-7666. https://doi.org/10.1029/98JC02622
4. Bruun P (1962) Sea-level rise as a cause of shore erosion. J Waterw Harb Div 88(1): 117-130. https://doi.org/10.1061/JWHEAU.0000252
5. Church JA, Clark PU, Cazenave A et al. (2013) Sea level change. PM Camb Univ Press. http://drs.nio.org/drs/handle/2264/4605
6. Dalrymple RW, Choi K (2007). Morphologic and facies trends through the fluvial–marine transition in tide-dominated depositional systems: a schematic framework for environmental and sequence-stratigraphic interpretation. Earth-Sci Rev 81(3-4): 135-174. https://doi.org/10.1016/j.earscirev.2006.10.002
7. Dastgheib A, Martinez C, Udo K et al (2021) Climate change driven shoreline change at Hasaki Beach Japan: A novel application of the Probabilistic Coastline Recession (PCR) model. Coast Eng: 104079. https://doi.org/10.1016/j.coastaleng.2021.104079
8. De Swart HE, Zimmerman JTF (2009) Morphodynamics of tidal inlet systems. Annu Rev Fluid Mech41: 203-229. https://doi.org/10.1146/annurev.fluid.010908.165159
9. Dissanayake DMPK, Ranasinghe R, Roelvink JA (2012) The morphological response of large tidal inlet/basin systems to relative sea level rise. Clim Chang 113(2): 253-276. https://doi.org/10.1007/s10584-012-0402-z
10. Duong TM, Ranasinghe R, Walstra D et al (2016) Assessing climate change impacts on the stability of small tidal inlet systems: Why and how?. Earth-Sci Rev 154: 369-380. https://doi.org/10.1016/j.earscirev.2015.12.001
11. Duong TM, Ranasinghe R, Luijendijk A et al (2017) Assessing climate change impacts on the stability of small tidal inlets: Part 1-Data poor environments. Mar Geol 390: 331-346. https://doi.org/10.1016/j.margeo.2017.05.008
12. Duong TM, Ranasinghe R, Thatcher M et al (2018) Assessing climate change impacts on the stability of small tidal inlets: Part 2-Data rich environments. Mar Geol 395: 65-81. https://doi.org/10.1016/j.margeo.2017.09.007
13. Edmonds DA, Slingerland RL (2007) Mechanics of river mouth bar formation: Implications for the morphodynamics of delta distributary networks. J Geophys Res: Earth Surf: 112(F2). https://doi.org/10.1029/2006JF000574
14. Fan X, Miao C, Duan Q, et al (2020) The performance of CMIP6 versus CMIP5 in simulating temperature extremes over the global land surface. J Geophys Res: Atmos 125(18), e2020JD033031. https://doi.org/10.1029/2020JD033031
15. Gochis DJ, Barlage M, Cabell R et al (2020) The WRF-Hydro® modeling system technical description, (Version 5.1.1). NCAR Technical Note. https://doi.org/10.5281/zenodo.3625238
16. Gochis DJ, Yu Y, Yates DN (2015) The WRF-Hydro model technical description and user's guide, version 3.0. NCAR Technical Doc.

https://ral.ucar.edu/sites/default/files/public/WRF_Hydro_User_Guide_v3.0_CLEAN.pdf

17. Gregory JM, Griffies SM, Hughes CW et al (2019) Concepts and Terminology Sea Level: Mean, Variability and Change, Both Local and Global. Surv Geophys 40:1251-1289. https://doi.org/10.1007/s10712-019-09525-z
18. Guo L, Van der Wegen M, Roelvink JA et al (2014) The role of river flow and tidal asymmetry on 1-D estuarine morphodynamics. J Geophys Res: Earth Surf 119(11): 2315-2334. https://doi.org/10.1002/2014JF003110
19. Harada M, Maruya Y, Kojima T et al (2020) Flood Frequency Analysis and Impact Assessment for Climate Change in the Nagara River Basin. J JSCE 8(1): 79-86. https://doi.org/10.2208/journalofjsce.8.1_79
20. Harris PT, Heap AD, Bryce SM et al (2002) Classification of Australian clastic coastal depositional environments based upon a quantitative analysis of wave, tidal, and river power. J Sediment Res 72(6): 858-870. https://doi.org/10.1306/040902720858
21. Hirabayashi Y, Mahendran R, Koirala S et al (2013) Global flood risk under climate change. Nat Clim Chang 3(9): 816-821. https://doi.org/10.1038/nclimate1911
22. Hong SY, Dudhia J, Chen SH (2004) A revised approach to ice microphysical processes for the bulk parameterization of clouds and precipitation. *Mon Wea Rev* **132:** 103-120. https://doi.org/10.1175/1520-0493(2004)132<0103:ARATIM>2.0.CO;2
23. Hong SY, Lim, JOJ (2006) The WRF single–moment 6–class microphysics scheme (WSM6), *J Korean Meteor Soc* **42**: 129-151.
24. Jeworrek J, West G, Stull R (2021) WRF Precipitation Performance and Predictability for Systematically Varied Parameterizations over Complex Terrain. Wea Forecasting 36(3): 893-913. https://doi.org/10.1175/WAF-D-20-0195.1
25. Kim YH, Min SK, Zhang X et al (2020) Evaluation of the CMIP6 multi-model ensemble for climate extreme indices. Wea Clim Extrem 29: 100269. https://doi.org/10.1016/j.wace.2020.100269
26. Kimura F Kitoh A (2007) Downscaling by pseudo global warming method. Final Rep ICCAP, 43-46.
27. Kobayashi K, Tanaka T, Shinohara M et al (2020) Analyzing Future Changes of Extreme River Discharge in Japan using d4PDF. J Jpn Soc Civ Eng Ser B1 Hydraul Eng 76(1): 140-152. https://doi.org/10.2208/jscejhe.76.1_140
28. Le Cozannet G, Bulteau T, Castelle B et al (2019) Quantifying uncertainties of sandy shoreline change projections as sea level rises. Sci Rep 9(1): 1-11. https://doi.org/10.1038/s41598-018-37017-4
29. Leonardi N, Canestrelli A, Sun T et al (2013) Effect of tides on mouth bar morphology and hydrodynamics. J Geophys Res: Oceans 118(9): 4169-4183. https://doi.org/10.1002/jgrc.20302
30. Leuven JRFW, Pierik HJ, Vegt Mvd et al (2019) Sea-level-rise-induced threats depend on the size of tide-influenced estuaries worldwide. Nat Clim Chang 9: 986-992. https://doi.org/10.1038/s41558-019-0608-4

31. Liu C, Ikeda K, Thompson G et al (2011) High-Resolution Simulations of Wintertime Precipitation in the Colorado Headwaters Region: Sensitivity to Physics Parameterizations. Mon Wea Rev 139(11): 3533-3553. https://doi.org/10.1175/MWR-D-11-00009.1
32. Ohizumi K, Ishibashi K, Nakamura R et al (2021) Quantification of processes of morphological changes by numerical simulation and elucidation of flushing mechanism at Arakawa river mouth sandbar in Niigata. J Jpn Soc Civ Eng Ser B3 Ocean Eng 77(2):355-360. https://doi.org/10.2208/jscejoe.77.2_I_355
33. Osakada Y, Nakakita E (2018) Future Change of Occurrence Frequency of Baiu Heavy Rainfall and Its Linked Atmospheric Patterns by Multiscale Analysis. SOLA 14:79-85. https://doi.org/10.2151/sola.2018-014
34. Sandwell DT, Müller RD, Smith WH et al (2014) New global marine gravity model from CryoSat-2 and Jason-1 reveals buried tectonic structure. Sci 346(6205): 65-67. https://www.science.org/doi/10.1126/science.1258213
35. Sato T, Kimura, F Kitoh A (2006) Projection of global warming onto regional precipitation over Mongolia using a regional climate model. J Hydrol 333:144-154. https://doi.org/10.1016/j.jhydrol.2006.07.023
36. Shimura T, Mori N (2019) Future Projection of Spectral Wave Climate around Japan. J Jpn Soc Civ Eng Ser B2 Coast Eng 75(2): I_1177-I_1182. https://doi.org/10.2208/kaigan.75.I_1177
37. Skamarock WC, Klemp JB, Duddhia J et al. (2008) A description of the advanced research WRF version 3, NCAR Technical Note. https://doi.org/10.5065/D68S4MVH
38. Sutherland J, Peet AH, Soulsby RL (2004) Evaluating the performance of morphological models. Coast Eng 51(8-9): 917-939. https://doi.org/10.1016/j.coastaleng.2004.07.015
39. Thompson G, Field PR, Rasmussen RM (2008) Explicit Forecasts of Winter Precipitation Using an Improved Bulk Microphysics Scheme. Part II: Implementation of a New Snow Parameterization. *Mon Wea Rev* **136**: 5095–5115. https://doi.org/10.1175/2008MWR2387.1
40. Trenberth KE (2011) Changes in precipitation with climate change. Clim Res 42(1-2): 123-138. https://doi.org/10.3354/cr00953
41. Mäll M, Nakamura R, Suursaar Ü et al (2020) Pseudo-climate modelling study on projected changes in extreme extratropical cyclones, storm waves and surges under CMIP5 multi-model ensemble: Baltic Sea perspective. Nat Hazards 102(1):67-99. https://doi.org/10.1007/s11069-020-03911-2
42. Mohan PR, Srinivas CV, Yesubabu V et al (2018) Simulation of heavy rainfall event over Chennai in Southeast India using WRF: Sensitivity to microphysics parameterization. Atmos Res 210 (15): 83-99. https://doi.org/10.1016/j.atmosres.2018.04.005
43. Mori N, Nakajo S, Iwamura S et al (2018) Projection of decrease in Japanese beaches due to climate change using a geographic database. Coast Eng J 60(2): 239-246. https://doi.org/10.1080/21664250.2018.1488513
44. Mori N, Takemi T, Tachikawa Y et al (2021) Recent nationwide climate change impact assessments of natural hazards in Japan and East Asia. Wea Clim Extrem 32: 100309.

https://doi.org/10.1016/j.wace.2021.100309

45. Morim J, Hemer M, Wang LX et al (2019) Robustness and uncertainties in global multivariate wind-wave climate projects. Nat Clim Chang 9(10): 1-8. https://doi.org/10.1038/s41558-019-0542-5
46. Nakamura R, Mäll M (2021) Pseudo Global Warming Sensitivity Experiments of Subtropical Cyclone Anita (2010) Under RCP 8.5 Scenario. J Geophys Res: Atmos 126(24): e2021JD035261. https://doi.org/10.1029/2021JD035261
47. Nakamura R, Shibayama T, Esteban M et al (2016) Future typhoon storm surges under different global warming scenario: case study of typhoon Haiyan (2013). Nat Hazards 82(3):1645-1681. https://doi.org/10.1007/s11069-016-2259-3
48. Nakamura R, Shibayama T, Esteban M et al (2020) Simulations of future typhoons and storm surges around Tokyo Bay using IPCC AR5 RCP 8.5 scenario in multi global climate models. Coast Eng J 62(1): 101-127. https://doi.org/10.1080/21664250.2019.1709014
49. Nienhuis JH, Ashton AD, Nardin W et al (2016) Alongshore sediment bypassing as a contral on river mouth morphodynamics. J Geophys Res: Earth Surf 121(4): 664-683. https://doi.org/10.1002/2015JF003780
50. Ranasinghe R, Callaghan D, Stive MJ (2012) Estimating coastal recession due to sea level rise: beyond the Bruun rule. Clim Chang 110(3): 561-574. https://doi.org/10.1007/s10584-011-0107-8
51. Ranasinghe R, Duong TM, Uhlenbrook S, et al. (2013) Climate-change impact assessment for inlet-interrupted coastlines. Nat Clim Chang 3(1): 83-87. https://doi.org/10.1038/nclimate1664
52. Ranasinghe R (2016) Assessing climate change impacts on open sandy coasts: A review. Earth-Sci Rev 160: 320-332. https://doi.org/10.1016/j.earscirev.2015.12.001
53. Roelvink D, Reniers A, Van Dongeren A et al (2009) Modelling storm impacts on beaches, dunes and barrier islands. Coast Eng 56:1133-1152. https://doi.org/10.1016/j.coastaleng.2009.08.006
54. Udo K, Takeda Y (2017) Projections of future beach loss in Japan due to sea-level rise and uncertainties in projected beach loss. Coast Eng J 59(02): 1740006. https://doi.org/10.1142/S057856341740006X
55. Van der Wegen M, Roelvink JA (2012) Reproduction of estuarine bathymetry by means of a process-based model: Western Scheldt case study, the Netherlands. Geomorphol 179(15): 152-167. https://doi.org/10.1016/j.geomorph.2012.08.007
56. Van Rijn LC, Walstra DJR, Grasmeijer B et al (2003) The predictability of cross-shore bed evolution of sandy beaches at the time scale of storms and seasons using process-based Profile models. Coast Eng 47(3): 295-327. https://doi.org/10.1016/S0378-3839(02)00120-5
57. Yoshida J, Udo K, Takeda Y et al. (2013) Potential impact of climate change at five Japanese beaches. J Coast Res 65: 2185-2190. https://doi.org/10.2112/SI65-369.1
58. Vousdoukas MI, Ranasinghe R, Mentaschi L et al (2020) Sandy coastlines under threat of erosion. Nat Clim Chang 10: 260-263. https://doi.org/10.1038/s41558-020-0697-0

59. Wang J, Wang C, Rao V et al (2019) A parallel workflow implementation for PEST version 13.6 in high-performance computing for WRF-Hydro version 5.0: a case study over the midwestern United States. Geosci Dev 12(8): 3523-3539. https://doi.org/10.5194/gmd-12-3523-2019
60. Yamazaki D, Togashi S, Takeshima A et al (2018) High-Resolution Flow Direction Map of Japan. J Jpn Soc Civ Eng Ser B1 Hydraul Eng 74(5): I_163-I_168. https://doi.org/10.2208/jscejhe.74.5_I_163
61. XBeach Documentation (2017) XBeach Documentation, Release pre-1.22.4344. https://oss.deltares.nl/documents/48999/1388930/Documentation+XBeach-v1.23.5387-XBeachX_BETA.pdf
62. Xie SP, Deser C, Vecchi GA et al (2015) Towards predictive understanding of regional climate change. Nat Clim Chang 5: 921-930. https://doi.org/10.1038/nclimate2689

Tables

Table.1 Cases of numerical simulations

WRF-Hydro version 5.1.1 (Gochis et al. 2020)			
Case	**Climate**	**Micro Physics Schemes**	
WSM5	Present	WRF Single-Moment 5-class (Hong et al. 2004)	
WSM5-SSP585	SSP585		
WSM5-RCP85	RCP85		
WSM6	Present	WRF Single-Moment 6-class (Hong et al. 2006)	
WSM6-SSP585	SSP585		
WSM6-RCP85	RCP85		
Thom	Present	Thompson (Thompson et al. 2008)	
Thom-SSP585	SSP585		
SWAN41.20AB			
Case	**Climate**	**Wind boundary condition**	**Water level boundary condition**
WSM5	Present	the simulated result of WRF-Hydro (WSM5)	0 m
WSM5-SSP585	SSP585	the simulated result of WRF-Hydro (WSM5-SSP585)	+ 0.33 m
WSM6	Present	the simulated result of WRF-Hydro (WSM6)	0 m
WSM6-SSP585	SSP585	the simulated result of WRF-Hydro (WSM6-SSP585)	+ 0.33 m
WSM6-RCP85	RCP85	the simulated result of	+ 0.39 m

		WRF-Hydro (WSM6-RCP85)		
XBeach				
Case	**Climate**	**Wave boundary condition**	**Water level boundary condition**	**Discharge boundary condition**
WSM5	Present	the simulated result of SWAN (WSM5)	0 m	the observed discharge (Tsudurayama stream gauging station)
WSM6	Present	the simulated result of SWAN (WSM6)	0 m	the observed discharge (Tsudurayama stream gauging station)
SSP585-SLR	SSP585	the simulated result of SWAN (WSM6)	+ 0.33 m	the observed discharge (Tsudurayama stream gauging station)
SSP585-SLR-WC	SSP585	the simulated result of SWAN (WSM6-SSP585)	+ 0.33 m	the observed discharge (Tsudurayama stream gauging station)
SSP585-SLR-WC-DC1	SSP585	the simulated result of SWAN (WSM6-SSP585)	+ 0.33 m	Future scenario DC1 (All periods of the observed discharge multiplied by 1.15)
SSP585-SLR-WC-DC2	SSP585	the simulated result of SWAN (WSM6-SSP585)	+ 0.33 m	Future scenario DC2 (At the time of maximum observed discharge in 20:00 17th May added by +491.04 m^3/s)
RCP85-SLR-WC-DC3	RCP85	the simulated result of SWAN (WSM6-RCP85)	+ 0.39 m	Future scenario DC3 (At the time of maximum observed discharge in 20:00 17th May added by +34.30 m^3/s)

Table.2 Quantitative assessment and results of BSS

BSS (Sutherland et al. 2004)						
Excellent		1.0-0.5				
Good		0.5-0.2				
Reasonable/fair		0.2-0.1				
Poor		0.1-0				
Bad		<0				
The results of BSS						
Line		A1	C1	C2	C3	C4
Case	WSM5	0.3834	0.4132	-0.4361	-0.5502	0.5046
	WSM6	0.4071	0.4711	-0.3534	-0.5712	0.4986

Figures

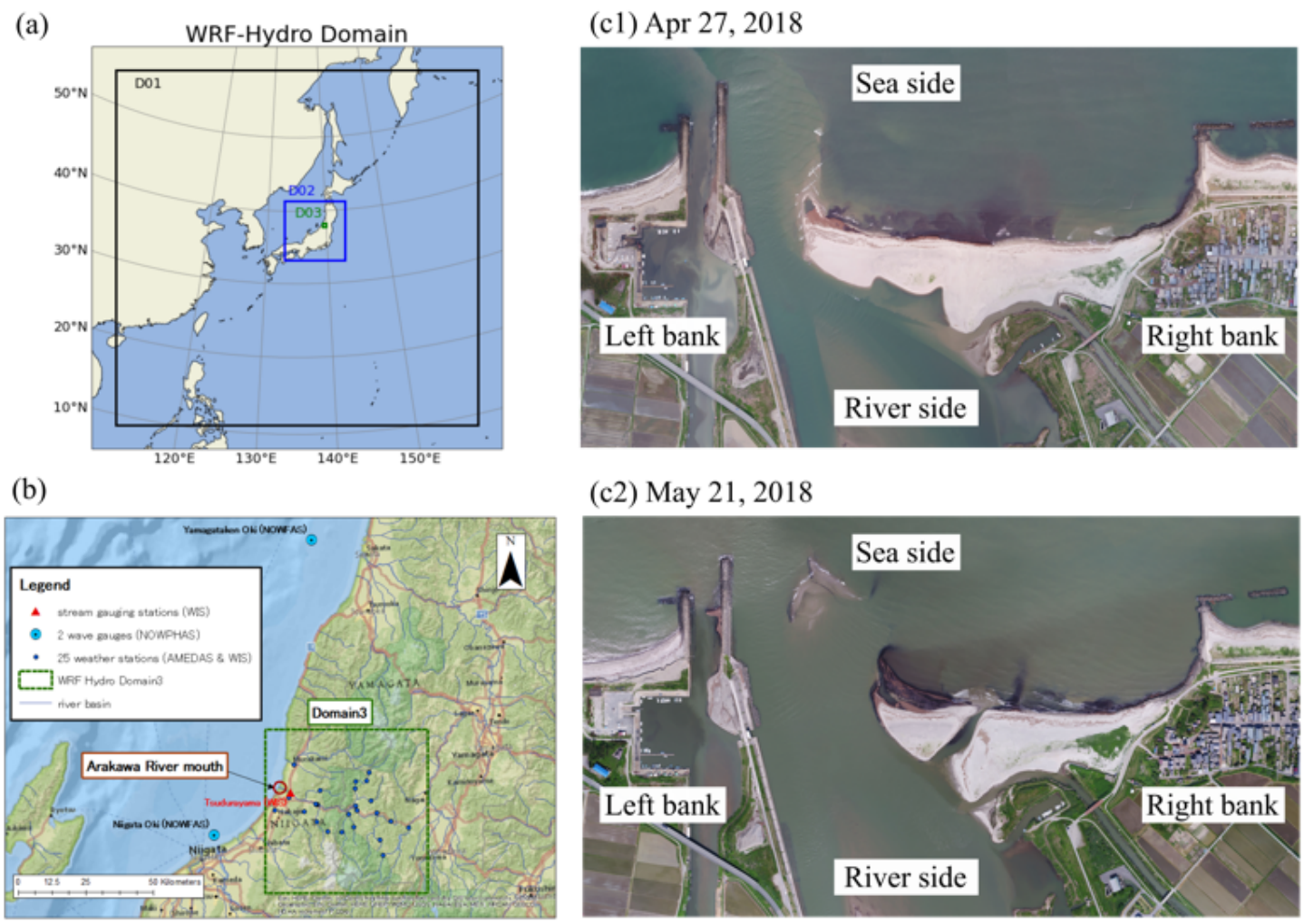

Figure 1

Location of Arakawa River mouth in the study area; (a) is WRF-Hydro Domain (D01–D03); (b) is the area of hydrological simulation conducted by WRF-Hydro (Domain3); (b) also illustrates the observed points of the stream gauging station (WIS), wave gauges (NOWPHAS), and weather stations (AMEDAS, WIS); (c) is the aerial photogrammetry taken on April 27 and May 21 at the Arakawa River mouth

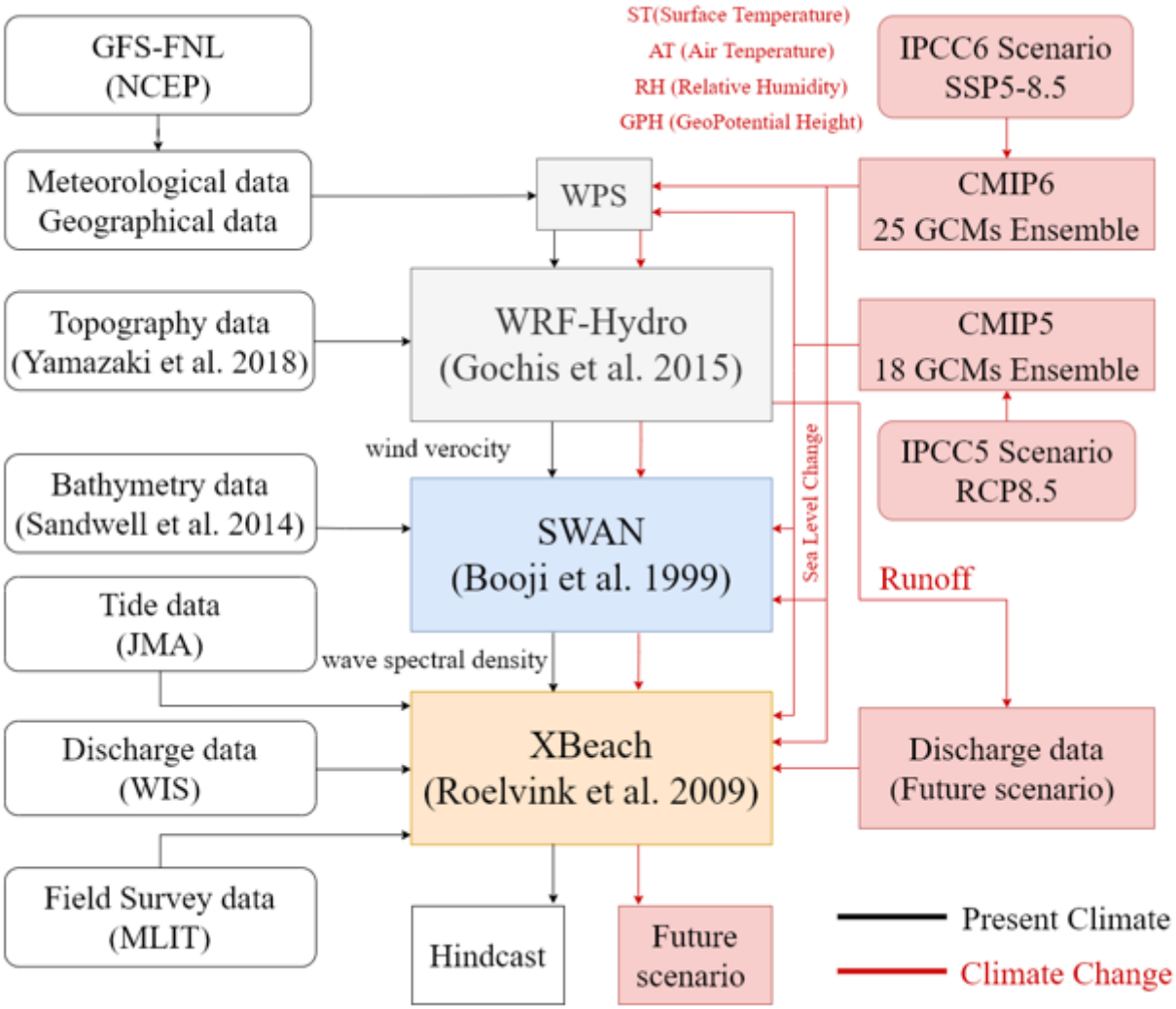

Figure 2

Configuration of numerical modelling system; black arrows indicate numerical simulation flow under present climate; red arrows indicate numerical simulation flow under climate change

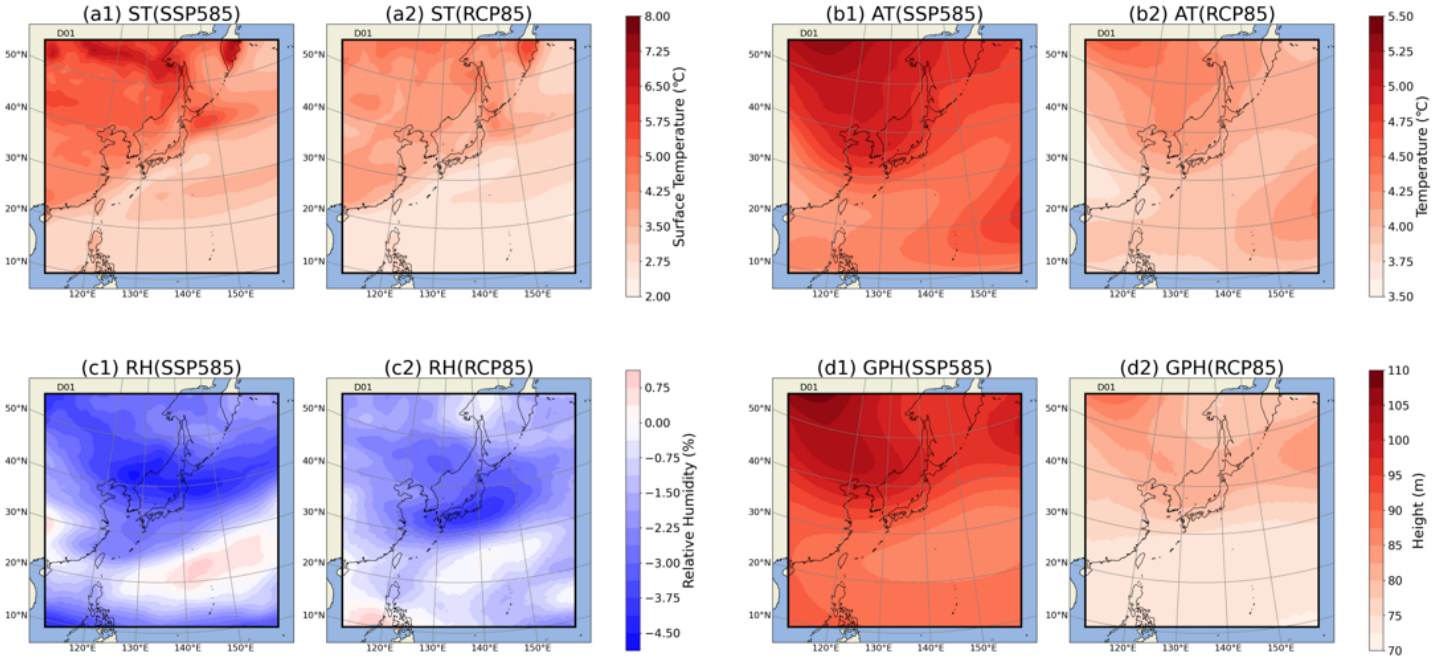

Figure 3

Difference between future (2081–2100) and present period (2015–2024) from each multi-model ensemble; (a) is ST, (b) is AT, (c) is RH, (d) is GPH; each PGW fields is based on SSP585 and RCP85

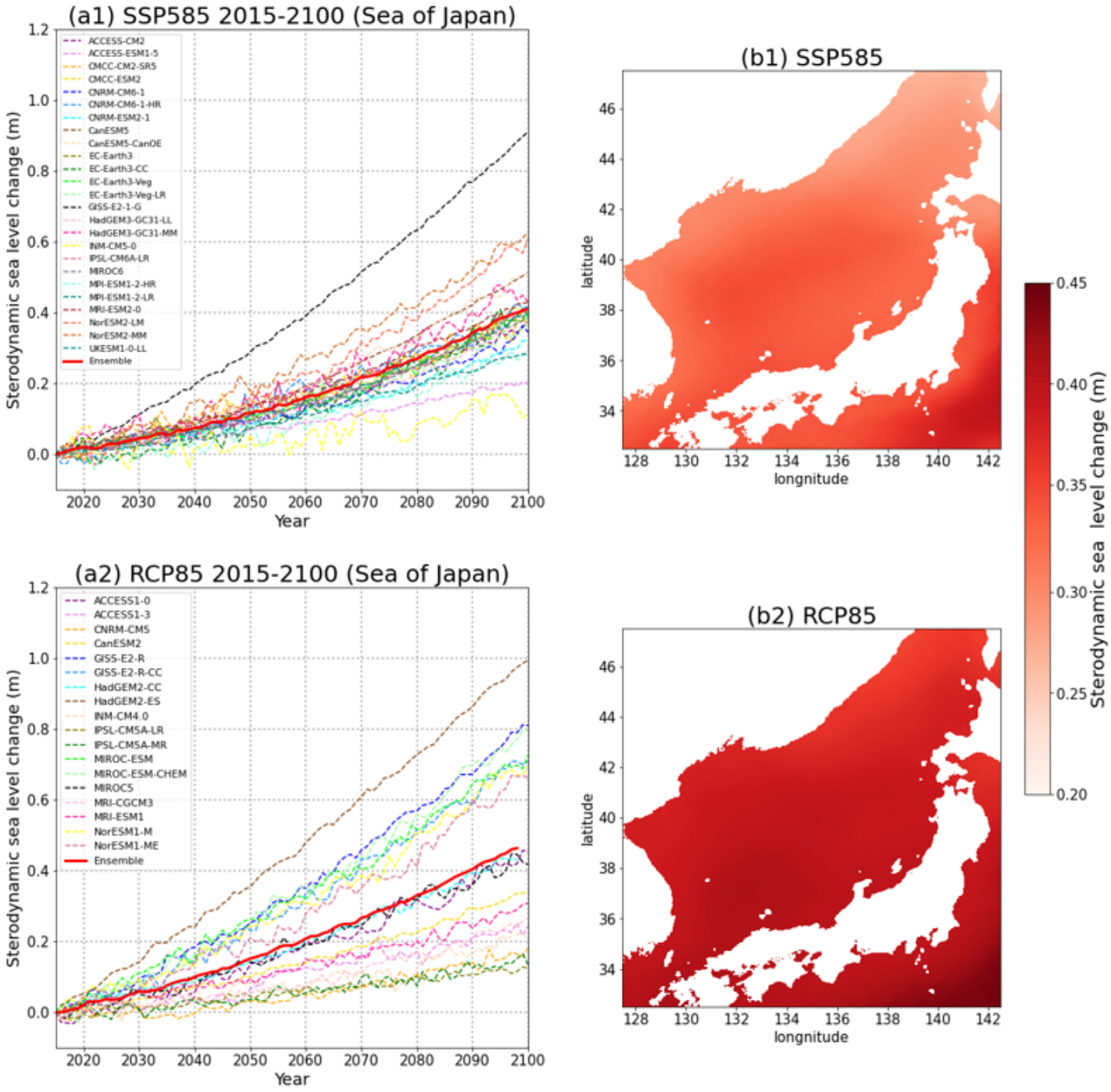

Figure 4

Sterodynamic sea level change around the Sea of Japan; evaluation range is same as the domain simulated by SWAN; (a) is annual mean sea level change from 2015–2100; (b) is difference of sea level change between future (2081–2100) and present period (2015–2024) from each multi-model ensemble in May

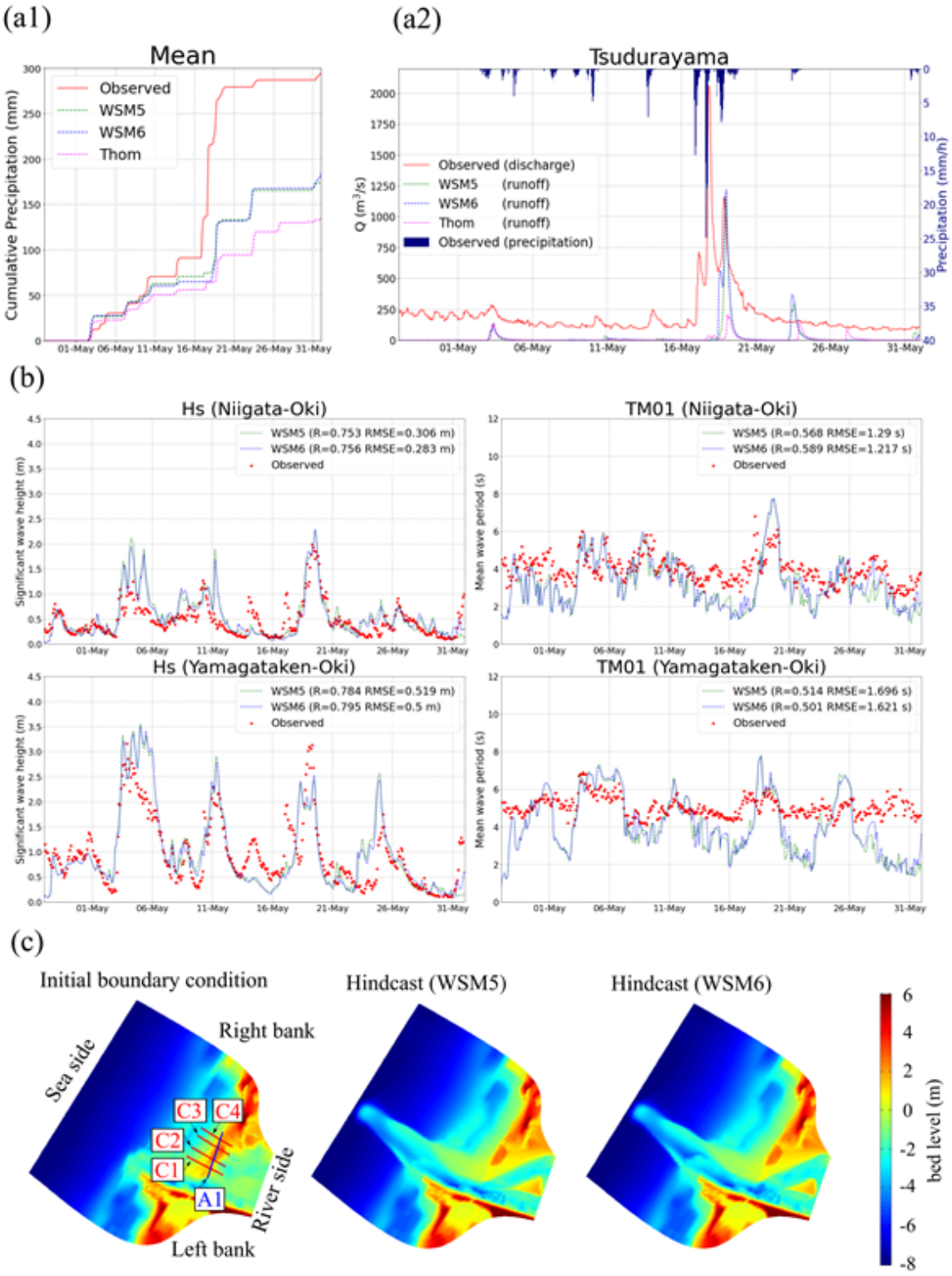

Figure 5

Numerical simulation results under present climate; (a1) is simulated and observed cumulative precipitation in Arakawa River basin, observed value is the mean of 25 weather stations (Figure 1 (b)); (a2) is the simulated runoff and observed discharge in Tsudurayama stream gauging station (Figure 1 (b)); (b) is the simulated and observed values of the significant wave heights and mean wave periods, the

two observed locations are illustrated in Figure 1 (b); (c) is the initial boundary condition and hindcast simulation of XBeach

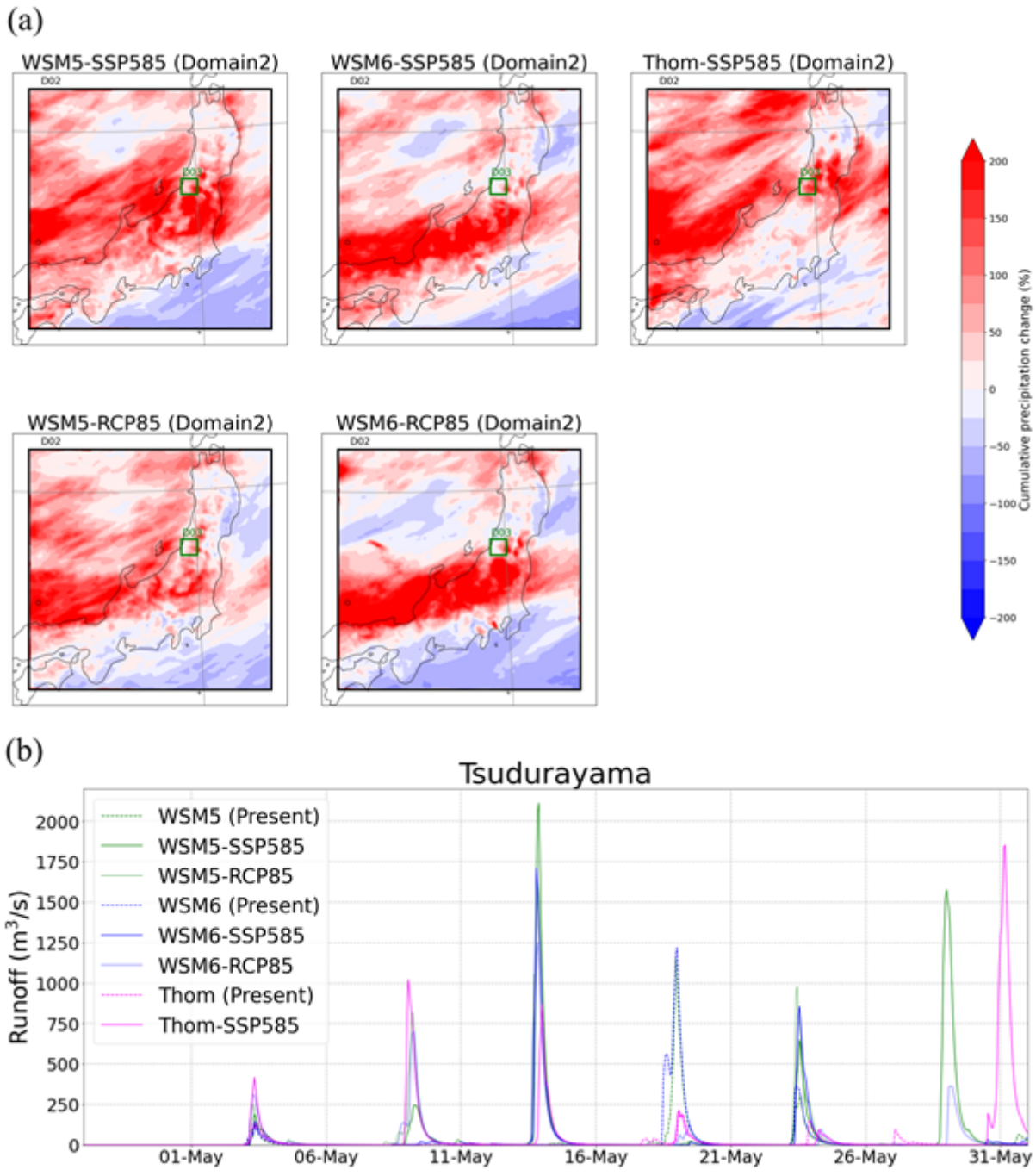

Figure 6

Comparison of precipitation and runoff between future and present climate; (a) is the change rate of cumulative precipitation between future scenarios and hindcast; (b) is the simulated runoff in future scenarios and hindcast

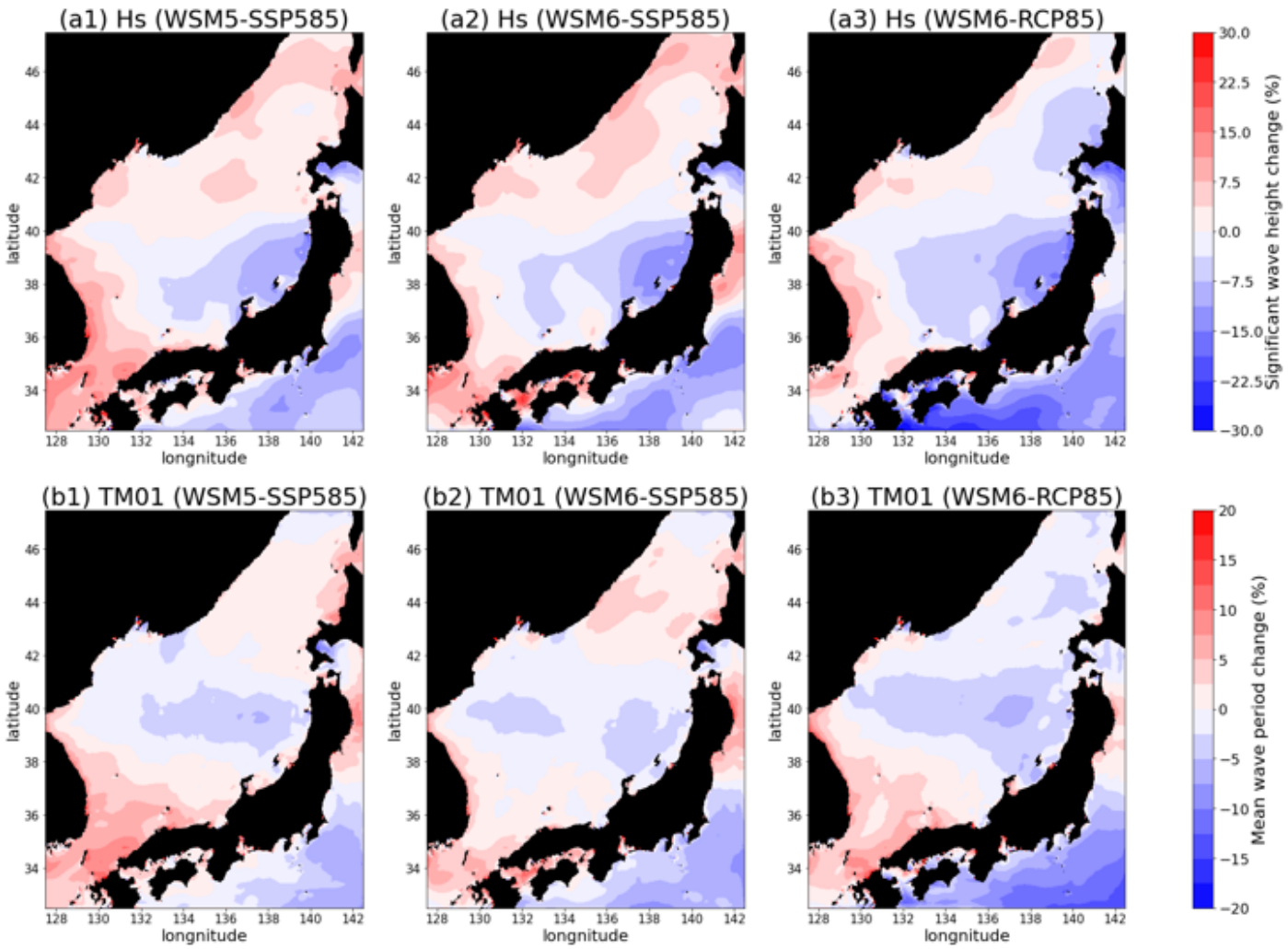

Figure 7

Comparison of wave fields between future and present climate; (a) change of significant wave height averaged in this period between future scenarios and hindcast; (b) change of mean wave period averaged in this period between future scenarios and hindcast

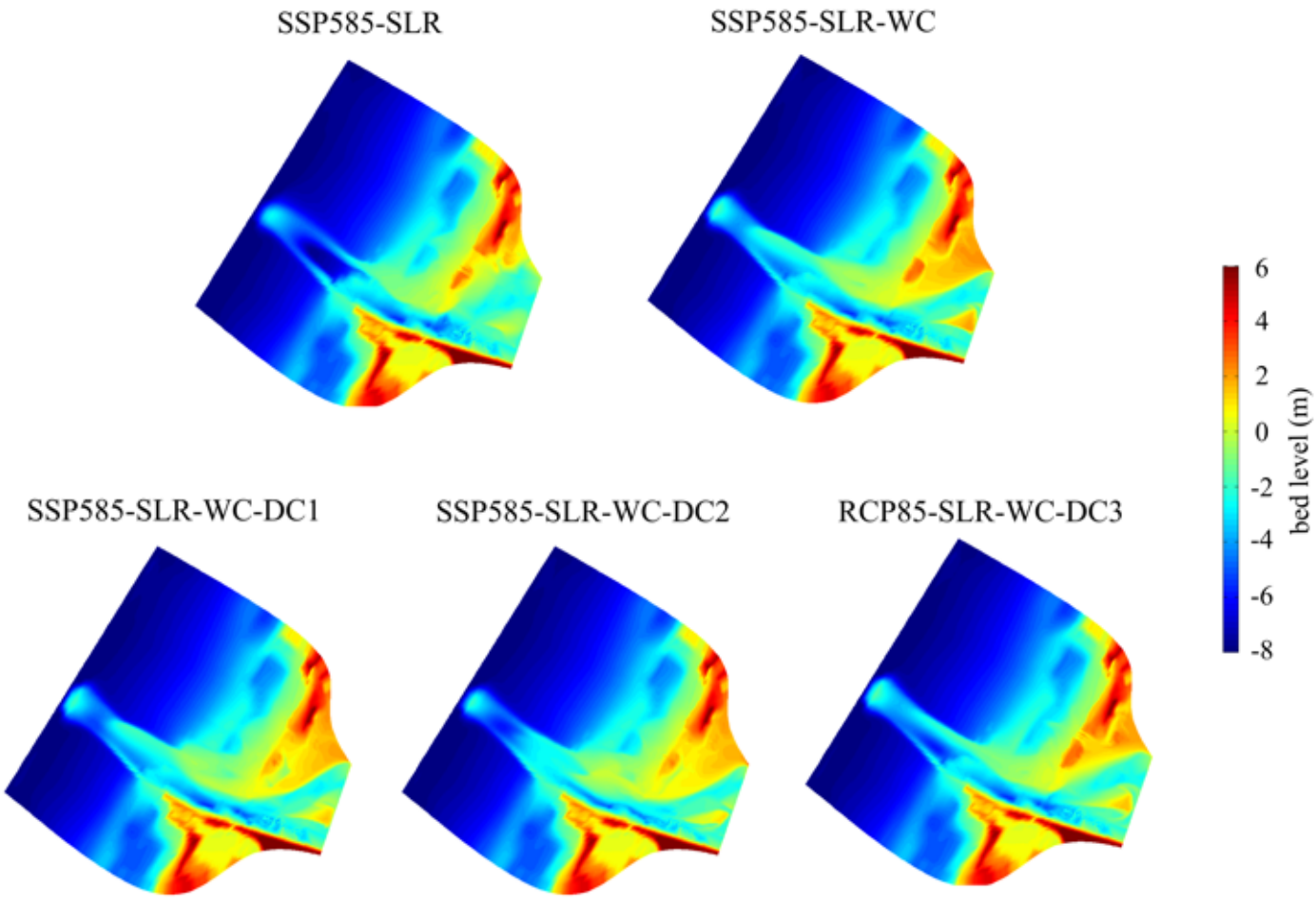

Figure 8

Numerical simulation results under climate change

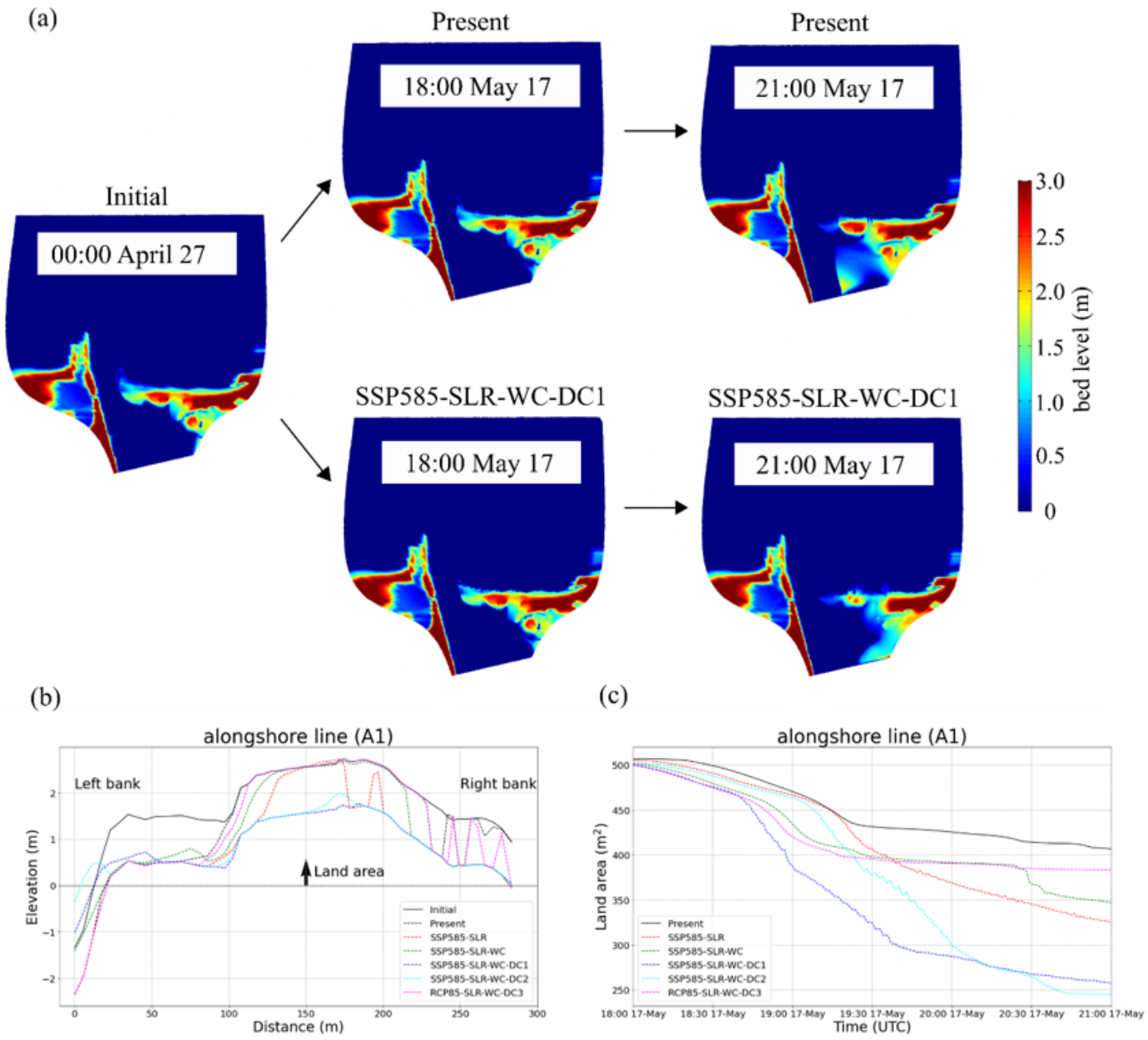

Figure 9

Numerical simulation results focusing on sandbar; (a) is the time series change of the results under the present and future climate, including at the maximum discharge (20:00 UTC, May 17), when maximum discharges of hindcast and SSP585-SLR-WC-DC1 are 2063.27 m^3/s and 2373.35 m^3/s, respectively; (b) shows the cross-sectional line on the A1 of each case at 00:00 UTC, May 31; (c) shows time series of the land cross-sectional area illustrated in (b); in (c), when the land area is decreasing, the sandbar is interpreted as the opening due to change in morphology

Supplementary Files

This is a list of supplementary files associated with this preprint. Click to download.

- Supplementaryfile.docx